Effect of Silanization Film Thickness in Soft Lithography of Nanoscale Features

Lucas H. Ting
Shirin Feghhi
Sangyoon J. Han
Marita L. Rodriguez
Nathan J. Sniadecki

Department of Mechanical Engineering,
University of Washington,
Seattle, WA 98195

Soft lithography was used to replicate nanoscale features made using electron beam lithography on a polymethylmethacrylate (PMMA) master. The PMMA masters were exposed to fluorinated silane vapors to passivate its surfaces so that polydimethylsiloxane (PDMS) did not permanently bond to the master. From scanning electron microscopy, the silanization process was found to deposit a coating on the master that was a few hundreds of nanometers thick. These silane films partially concealed the nanoscale holes on the PMMA master, causing the soft lithography process to produce PDMS features with dimensions that were significantly reduced. The thickness of the silane films was directly measured on silicon or PMMA masters and was found to increase with exposure time to silane vapors. These findings indicate that the thickness of the silane coatings is a critical parameter when using soft lithography to replicate nanoscale features, and caution should be taken on how long a master is exposed to silane vapors.
[DOI: 10.1115/1.4005665]

Keywords: silane, soft lithography, PDMS, PMMA, e-beam lithography

1 Introduction

Soft lithography is a set of fabrication methods, in which an elastomeric polymer is cast against a master [1,2]. The master is made from silicon and photoresist and has surface features which are fabricated using lithography methods. PDMS is a polymer commonly used in soft lithography applications [1]. The advantage of soft lithography and PDMS is that it is relatively simple to replicate a device with nanoscale features without incurring additional costs in a clean-room [3]. Due to its ease of use, soft lithography has been applied to manufacture the channels in microfluidic platforms [4–6] or stamps for microcontact printing [7]. Since PDMS is biocompatible, it can also be used for applications with biological cells [8]. In particular, PDMS and soft lithography are crucial to manufacturing arrays of flexible posts for measuring cellular forces at the nanoscale [9]. The post arrays have helped to elucidate the role of cellular forces in migration, morphogenesis, mechanotransduction, and stem cell biology [10–16]. Despite these insights, there is a critical need to make these posts with even smaller dimensions [17]. However, it is unclear if PDMS and soft lithography are capable of manufacturing posts at the nanoscale [18,19].

In order to use PDMS, the surface of a master needs to be passivated in order to prevent irreversible bonding with PDMS. Masters are typically treated under vacuum with vapors from a fluorinated silane agent, which deposits a "nonstick" film on the master [3,20]. This silane film is particularly important if the master is made from silicon because it can form covalent bonds (Si–O–Si) with PDMS [3]. For masters made with electron beam (e-beam) lithography and PMMA photoresist, the need for passivation is less clear. Initial reports have suggested that PDMS does not bond irreversibly to PMMA [3]. However, PDMS has been bonded successfully to PMMA for microfluidic applications [21,22].

Here, we investigated whether e-beam lithography and PMMA could be used with PDMS and soft lithography to manufacture nanoscale features. A pattern of nanometer-sized holes was formed in PMMA masters and when PDMS was cast from the masters, the replica had positive features ("posts") that were significantly smaller than the dimensions of the original holes in the master. The dimensions of the holes were found to be reduced in size as a direct result of silanization, which deposited a silane film that backfilled the PMMA hole. The main finding of this work is that silane coatings can adversely affect the nanoscale dimensions of the PDMS structures made with soft lithography.

2 Materials and Methods

2.1 E-Beam Lithography. All features were created on 4-in. ⟨100⟩ oriented silicon wafers (Silicon Quest Intl.). The wafers were spin coated with 495PMMA A11 resist (MicroChem Corp.) at 1000 rpm for 4 min for a film thickness of 1.9 μm or with 495PMMA A4 resist at 2500 rpm for 1.5 min for a film thickness of 200 nm. After spin coating, the resist was cured at 180 °C for 4 min to evaporate the solvent inside the photoresist. E-beam patterns were designed using KLAYOUT CAD software and then written using a JEOL JBX-6300FS system with a beam intensity dosage of 750 μC. After writing, the wafers were developed in a solution with a 1:1 ratio of methyl isobutyl ketone (Sigma) and isopropyl alcohol (Sigma) for 2 min. The wafers were then dried with nitrogen.

2.2 Plasma Treatment and Silane Deposition. The PMMA masters were treated with plasma to activate the surface using a plasma chamber (Plasma prep II, SPI) for 1.5 min at a pressure of 0.3 mbar, current of 100 mA, and power of 100 W. The masters were placed inside a plastic desiccator and a 5–10 μl droplet of (tridecafluoro-1,1,2,2-tetrahydrooctyl)-1-trichlorosilane (T2492-KG, United Chemical Technologies) was placed on an aluminum tray that was placed at the center of the desiccator. The masters were arranged at equal distances from the tray to eliminate any effects from spatial variations. A vacuum was applied to the desiccator for 5 min so that the chamber pressure reached 0.35 bars. The valve of the desiccator was then closed and masters were kept under vacuum with silane vapor for 30 s, 1 h, or 18 h before removing them from the chamber.

2.3 PDMS Casting. Uncured PDMS was prepared by mixing its base and curing agent (Sylgard 184, Dow Corning) in a 10:1 ratio, and then degassing this mixture under vacuum pressure until

Manuscript received June 4, 2011; final manuscript received June 19, 2011; published online March 30, 2012. Assoc. Editor: Boris Khusid.

Copyright © 2011 by ASME

Downloaded 26 Apr 2012 to 128.95.104.109. Redistribution subject to ASME license or copyright; see http://www.asme.org/terms/Terms_Use.cfm

the air bubbles were removed. After degassing, the uncured PDMS was then poured onto the PMMA masters, and plasma-treated glass slides were placed on top of the PDMS in order to create a backing for the PDMS replicas as well as aid in the peeling process. The PDMS was then thermally cured in a gravity oven at 110 °C for 2 h. After curing, the glass-backing was slowly peeled away from the PMMA masters to release the cured PDMS.

2.4 Scanning Electron Microscopy. High resolution images were obtained from both PDMS and PMMA samples using a scanning electron microscope (SEM) (FEI Sirion). Since PDMS and PMMA are insulating materials, the samples were prepared for electron microscopy by fixing them onto a metal stand using carbon tape and painting them with carbon ink around the perimeter to increase the conductivity. A film of gold-palladium alloy was sputtered onto the samples to a target thickness of 7 nm. SEM imaging was done using a 2 kV accelerating voltage and with a working distance of 5 mm.

2.5 Profilometry. Bare samples of PMMA and silicon were silanized for 30 s, 1 h, or 18 h. A glass coverslip was placed on top of each sample to block half of the surface from silane deposition. After silanization, the glass was removed and the height of the silane film was measured using a profilometer (Alpha Step 200, Tencor). The scanning tip was brought into contact with the surface of the unsilanized portion of a sample and traced across the surface toward the deposited silane film. From the profilometer data, the change in height of the tip was used to measure the height of the silane film. The measurements were done using a 2 μm scanning length and had a vertical resolution of 5 nm. Tilt in the wafer was corrected using two reference points along the portion of the trace that was within the unsilanized region. Each sample was scanned at least 5 times across different portions of the interface between the silanized and unsilanized regions in order to obtain measurements of the average thickness of the silane film.

3 Results

3.1 PDMS Structures Have Smaller Dimensions Than PMMA Structures. E-beam lithography was used to create arrays of holes in a 1.9 μm thick layer of PMMA photoresist. The holes were designed to have 200 nm diameters, 3 μm spacing between the centers of the posts, and arranged in hexagonal packing. From inspection of the PMMA master under SEM, the holes fabricated with e-beam had diameters that were 290 ± 3 nm and were spaced 3 μm apart (Fig. 1). The arrays of holes in the PMMA master were suitable for testing whether soft lithography with PDMS is capable of replicating nanoscale features.

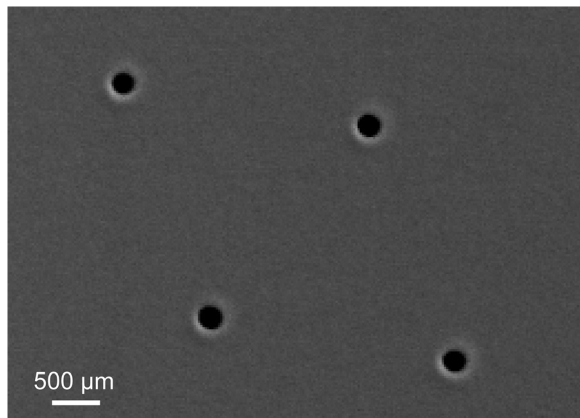

Fig. 1 SEM micrograph of a PMMA master. Holes were created in a 1.9 μm thick PMMA photoresist on a silicon wafer using e-beam lithography. The holes are arranged hexagonally, spaced 3 μm apart, and had an average diameter of 290 nm.

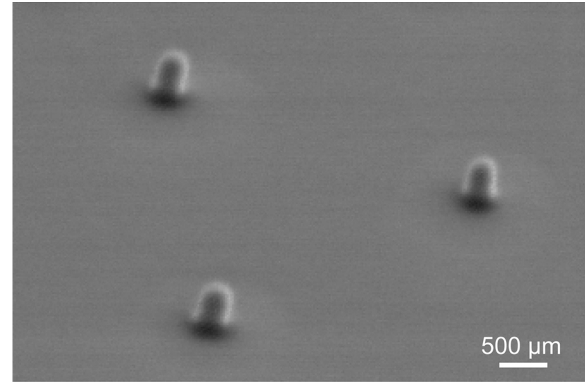

Fig. 2 SEM micrograph of PDMS nanoposts. PDMS was cast from the PMMA master shown in Fig. 1 after silanizing it for 1 h. The replica nanoposts had an average height of 465 nm and diameter of 227 nm, which are smaller than the dimensions of the master. View is at 45 deg off-vertical.

After the PMMA masters were treated with plasma for 90 s and silanized for 1 h, an array of nanoposts were made in PDMS by casting against the PMMA masters (Fig. 2). The diameters of the posts were 227 ± 6 μm, which was significantly less than the original dimensions of the holes in the PMMA master. Moreover, the heights of the posts were 465 ± 10 nm, which was significantly shorter than the thickness of the PMMA layer. These results indicated that the conventional process in soft lithography was not reliable in producing nanoscale PDMS structures that were the same size as the features on the master.

3.2 Plasma Erodes the PMMA Master but Silane Backfills the Holes. To understand the loss in dimensions during soft lithography, a group of three identical PMMA masters were made using e-beam lithography on a 200 μm thick film of PMMA resist. Holes in the masters were designed to be 50 nm in diameter. It was not possible to analyze the same sample after each processing step since a metal film needed to be sputtered onto the surface of the samples for SEM imaging. Instead, the samples were processed in the same batch and one master was removed from the group after e-beam fabrication, plasma treatment, or silanization and subsequently inspected under SEM.

From the micrographs taken, the diameters of the holes in the PMMA master after e-beam lithography were 58 ± 1 nm, which was slightly larger than the design of the layout (Fig. 3(*a*)). After plasma treatment, the diameters of the holes were measured to be 177 ± 4 nm (Fig. 3(*b*)). Plasma treatment likely caused the enlargement in the diameters by etching away PMMA with oxidative plasma [23]. After 1 h of silanization, the holes in the master were measured to be 119 ± 3 nm (Fig. 3(*c*)). Reduction in the diameter of the holes after silanization was likely due to deposition of a silane film onto the surface of the PMMA, which led to backfilling the holes.

3.3 Longer Deposition Time Causes a Loss in PDMS Dimensions. To examine the effect of silanization on the dimensions of PDMS structures cast from the masters, a set of holes with 280 ± 3 nm diameters and 1.9 μm depths were fabricated in PMMA. The PMMA masters were plasma treated and then silanized together in the same chamber. After 30 s, 1 h, or 18 h, one of the samples was removed from the batch and the chamber with the remaining masters was evacuated back to the original negative pressure. Each master was used to cast PDMS nanoposts, which were then examined under SEM. As a control, one sample was plasma treated, but was not silanized. PDMS did not permanently bond to the unsilanized PMMA master, but it was difficult to peel

Downloaded 26 Apr 2012 to 128.95.104.109. Redistribution subject to ASME license or copyright; see http://www.asme.org/terms/Terms_Use.cfm

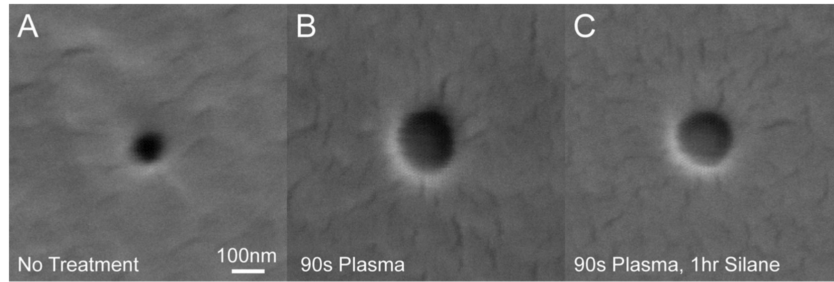

Fig. 3 SEM micrographs of PMMA masters after silanization process. Starting with (*a*) 200 nm deep PMMA resist, e-beam lithography was used to create 58 nm diameter holes. (*b*) The masters were then exposed to plasma for 90 s, which widened the holes to 177 nm. (*c*) They were then silanized for 1 h, which backfilled the holes and narrowed their diameters to 119 nm. The cracks observed on the surface are due to the sputtered metal film, which was needed for SEM imaging.

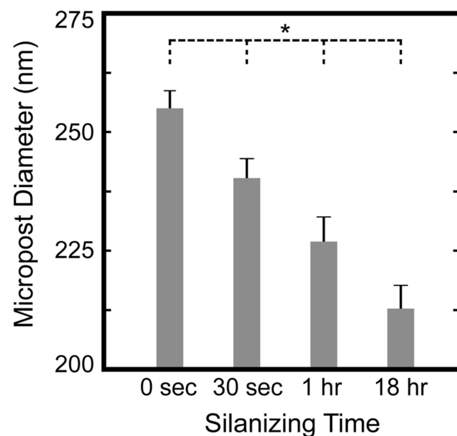

Fig. 4 Silanization time reduced nanopost diameter. A set of masters were created using e-beam lithography on 1.9 μm thick PMMA photoresist. The masters were plasma treated for 90 s and then silanized for 30 s, 1 h, or 18 h. The diameters of the nanoposts were measured from the SEM micrographs.

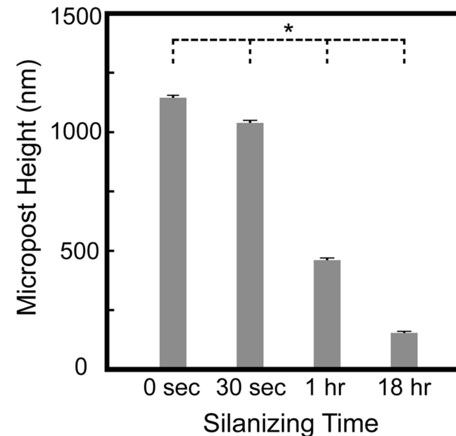

Fig. 5 Silanization time reduced nanopost height. The same set of PMMA masters as described in Fig. 4 were treated with plasma for 90 s and then silanized for 30 s, 1 h, or 18 h. The heights of the nanoposts were measured from the SEM micrographs.

the PDMS from the master. From SEM imaging, a large portion of the nanoposts were missing and were likely ripped-off during the peeling process. Measurements on these substrates were taken from the few regions where the nanoposts were still left intact.

The diameters of the nanoposts were observed to decrease in size with silanization time (Fig. 4). A one-way analysis of variance (ANOVA) with a Bonferroni's posthoc analysis was applied to the data and the diameters were found to have a statistically significant decrease with silanization time. Additionally, the heights of the PDMS posts were also observed to decrease in size with silanization time (Fig. 5). ANOVA and posthoc analysis revealed that the decrease in height was statistically significant for each time point. The nanoposts cast from a PMMA master that was silanized for 18 h were barely detectable under SEM and appeared as "stumps" (Fig. 6).

3.4 Measurement of Silane Deposition. To confirm that silane is capable of depositing a film with a substantial thickness onto a substrate, bare silicon and PMMA substrates were passivated. First, each substrate was treated with plasma for 90 s, and then silanized together in the same chamber. After each time point, a silicon and PMMA substrate were removed from the batch and the chamber was then evacuated back to negative pressure. The thickness of the silane films on the samples was measured on a profilometer (Fig. 7). From the measurements, silane thickness was confirmed to increase with exposure time to silane vapor. In addition, PMMA was found to have a higher propensity for silane deposition than silicon because it had the thickest films at each time point. After 30 s, there was a measureable film of silane on the PMMA surface, but the film on silicon was not detectable because its measurement was below the resolution of the profilometer. Overall, these results indicate that short silanization times are sufficient to passivate the surface of silicon or PMMA.

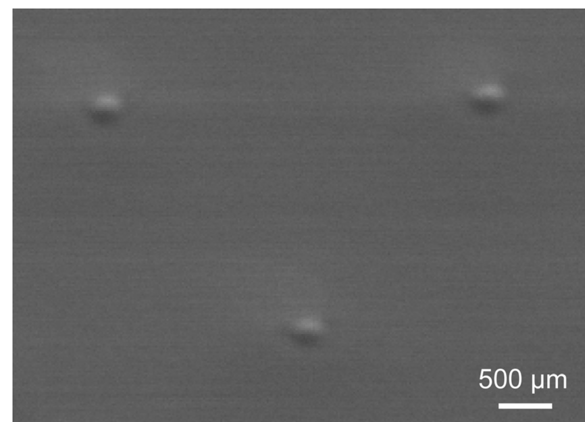

Fig. 6 SEM micrograph of PDMS nanoposts cast from a PMMA master silanized for 18 h. Due to silanization, nanoposts were small bumps, had reduced diameters, and almost negligible height. View is at 45 deg off-vertical.

Downloaded 26 Apr 2012 to 128.95.104.109. Redistribution subject to ASME license or copyright; see http://www.asme.org/terms/Terms_Use.cfm

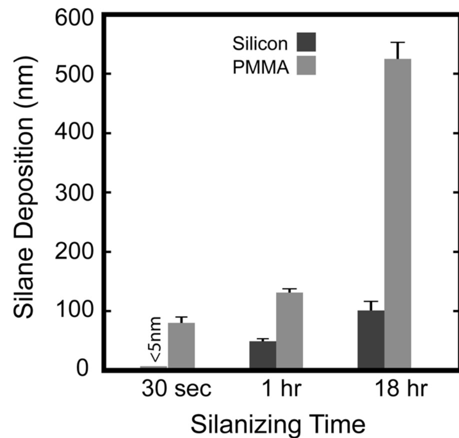

Fig. 7 Measurement of silane film thickness. Flat samples of silicon and PMMA were half-covered with a glass coverslip and silanized for 30 s, 1 h, or 18 h. The height of the deposited silane film was measured using a profilometer.

4 Discussion

Silanes are known to form self-assembled monolayers when dissolved in hexane and deposited onto a silicon or glass surface [24–26] The vapor phase silane used here formed a film that was substantially thicker than a single molecular layer, which suggests that the silane molecules arrange themselves in a disorganized fashion and with multiple layers. From visible inspection of vapor-deposited silane films on glass slides, there was an opaque, white-colored film that could not be removed with ethanol, isopropanol, acetone, or hexane. It could, however, be scratched away with a razor blade. The robustness of the silane film suggests that strong bonds hold the film together, but that there is weakness in the overall strength of the film, which is likely due to its disorganized arrangement.

From the measurements of the PDMS nanoposts, there was a large change in height with silanization time as compared to the change in diameter. From the SEM micrographs of the holes (Fig. 3), it was not clear whether there was a change in their depth after each processing step. However, if one compares the images of the holes after plasma treatment and after silanization (Figs. 3(*b*) and 3(*c*)), it can be determined qualitatively that there is a loss in depth after silanization by the different degree of shading at the bottom of the holes. Thus, it is likely that that there is anisotropic deposition of silane on PMMA; horizontal surfaces have a larger deposition rate while vertical surfaces have a lower deposition rate. It should be noted that a different variant of silane ((3-aminopropyl)trimethoxysilane) has been reported to diffuse into PMMA [27], so swelling of PMMA might contribute to the dimensional changes of the master. However, since the silane film was found to be thicker with silanization time, it is more likely that the film is grown on the surface.

Silane may not be completely necessary in soft lithography when using a PMMA master. In our control experiments, PDMS cast from an unsilanized PMMA master was difficult to peel, but it did not form irreversible bonds. However, many of the nanoposts were ripped off, which is likely because PDMS came in contact with the silicon surface at the bottom of the holes. Therefore, it is recommended that before PMMA is spun on a silicon wafer, a base coating should be applied so that PDMS does not bond directly to silicon. This base coating would also need to be relatively impervious to e-beam lithography so that it does not get removed during the direct-write process.

5 Conclusions

The main finding of this work is that silane coatings can adversely affect the nanoscale dimensions of PDMS structures made with soft lithography. Since a silicon wafer is typically used in combination with PMMA photoresist, it is a generally useful to passivate the entire master to prevent bonding between PDMS and silicon surfaces. However, silane deposition time should be closely monitored or else the features may not be properly replicated.

Acknowledgment

We would like to thank Richard Bojko for his assistance with e-beam lithography. This work was supported in part by Grants from National Science Foundation CAREER Award and the National Institutes of Health (HL097284, EB001650).

References

[1] Xia, Y. N., and Whitesides. G. M., 1998, Soft Lithography, Angew. Chem. Int. Ed., **37**, pp. 551–575.
[2] Whitesides, G. M., Ostuni, E., Takayama, S., Jiang, X., and Ingber, D. E., 2001, "Soft Lithography in Biology and Biochemistry," Annu. Rev. Biomed. Eng., **3**, pp. 335–373.
[3] Duffy, D. C., McDonald, J. C., Schueller, O. J. A., and Whitesides, G. M., 1998, "Rapid Prototyping of Microfluidic Systems in Poly(Dimethylsiloxane)," Analyt. Chem., **70**, pp. 4974–4984.
[4] McDonald, J. C., Duffy, D. C., Anderson, J. R., Chiu, D. T., Wu, H., Schueller, O. J., and Whitesides, G. M., 2000, "Fabrication of Microfluidic Systems in Poly(Dimethylsiloxane)," Electrophoresis, **21**, pp. 27–40.
[5] Sia, S. K., and Whitesides, G. M., 2003, "Microfluidic Devices Fabricated in Poly(Dimethylsiloxane) for Biological Studies," Electrophoresis, **24**, pp. 3563–3576.
[6] Quake, S. R., and Scherer, A., 2000, "From Micro- to Nanofabrication With Soft Materials," Science, **290**, pp. 1536–1540.
[7] Ruiz, S. A., and Chen, C. S., 2007, "Microcontact Printing: A Tool to Pattern," Soft Matter., **3**, pp. 168–177.
[8] Lee, J. N., Jiang, X., Ryan, D., and Whitesides, G. M., 2004, "Compatibility of Mammalian Cells on Surfaces of Poly(Dimethylsiloxane)," Langmuir, **20**, pp. 11684–11691.
[9] Tan, J. L., Tien, J., Pirone, D. M., Gray, D. S., Bhadriraju, K., and Chen, C. S., 2003, "Cells Lying on a Bed of Microneedles: An Approach to Isolate Mechanical Force," Proc. Natl. Acad. Sci. U.S.A., **100**, pp. 1484–1489.
[10] du Roure, O., Saez, A., Buguin, A., Austin, R. H., Chavrier, P., Siberzan, P., and Ladoux, B., 2005, "Force Mapping in Epithelial Cell Migration," Proc. Natl. Acad. Sci. U.S.A., **102**, pp. 2390–2395.
[11] Saez, A., Buguin, A., Silberzan, P., and Ladoux, B., 2005, "Is the Mechanical Activity of Epithelial Cells Controlled by Deformations or Rorces?" Biophys. J., **89**, pp. L52–L54.
[12] Cai, Y., Biais, N., Giannone, G., Tanase, M., Jiang, G., Hofman, J. M., Wiggins, C. H., Silberzan, P., Buguin, A., Ladoux, B., and Sheetz, M. P., 2006, "Nonmuscle Myosin IIA-Dependent Force Inhibits Cell Spreading and Drives F-Actin Flow," Biophys. J., **91**, pp. 3907–3920.
[13] Sniadecki, N. J., Anguelouch, A., Yang, M. T., Lamb, C. M., Liu, Z., Kirschner, S. B., Liu, Y., Reich, D. H., and Chen, C. S., 2007, "Magnetic Microposts as an Approach to Apply Forces to Living Cells," Proc. Natl. Acad. Sci. U.S.A., **104**, pp. 14553–14558.
[14] Nelson, C. M., Jean, R. P., Tan, J. L., Liu, W. F., Sniadecki, N. J., Spector, A. A., and Chen, C. S., 2005, "Emergent Patterns of Growth Controlled by Multicellular Form and Mechanics," Proc. Natl. Acad. Sci. U.S.A., **102**, pp. 11594–11599.
[15] Ruiz, S. A., and Chen, C. S., 2008, "Emergence of Patterned Stem Cell Differentiation Within Multicellular Structures," Stem Cells, **26**, pp. 2921–2927.
[16] Fu, J., Wang, Y. K., Yang, M. T., Desai, R. A., Yu, X., Liu, Z., and Chen, C. S., 2010, "Mechanical Regulation of Cell Function With Geometrically Modulated Elastomeric Substrates," Nat. Methods, **7**, pp. 733–736.
[17] Yang, M. T., Sniadecki, N. J., and Chen, C. S., 2007, "Geometric Considerations of Micro- to Nanoscale Elastomeric Post Arrays to Study Cellular Traction Forces," Adv. Mater., **19**, pp. 3119–3123.
[18] Roca-Cusachs, P., Rico, F., Martinez, E., Toset, J., Farre, R., and Navajas, D., 2005, "Stability of Microfabricated High Aspect Ratio Structures in Poly (Dimethylsiloxane)," Langmuir, **21**, pp. 5542–5548.
[19] Tooley, W. W., Feghhi, S., Han, S. J., Wang, J., and Sniadecki, N. J., 2011, "Fracture of Oxidized Polydimethylsiloxane During Soft Lithography of Nanopost Arrays," J. Micromech. Microeng., **21**, p. 054013.
[20] Chaudhury, M. K., and Whitesides, G. M., 1991, "Direct Measurement of Interfacial Interactions Between Semispherical Lenses and Flat Sheets of Poly (Dimethylsiloxane) and Their Chemical Derivatives," Langmuir, **7**, pp. 1013–1025.
[21] Ko, J. S., Yoon, H. C., Yang, H. S., Pyo, H. B., Chung, K. H., Kim, S. J., and Kim, Y. T., 2003, "A Polymer-Based Microfluidic Device for Immunosensing Biochips," Lab Chip., **3**, pp. 106–113.
[22] Chow, W. W. Y., Lei, K. F., Shi, G., Li, W. J., and Huang, Q., 2006, "Microfluidic Channel Fabrication by PDMS-Interface Bonding," Smart Mater. Struct., **15**, pp. S112–S116.

Downloaded 26 Apr 2012 to 128.95.104.109. Redistribution subject to ASME license or copyright; see http://www.asme.org/terms/Terms_Use.cfm

[23] Chai, J., Lu, F., Li, B., and Kwok, D. Y., 2004, "Wettability Interpretation of Oxygen Plasma Modified Poly(Methyl Methacrylate)," Langmuir, **20**, pp. 10919–10927.
[24] Sagiv, J., 1980, "Organized Monolayers by Adsorption 1. Formation and Structure of Oleophobic Mixed Monolayers on Solid-Surfaces," J. Am. Chem. Soc., **102**, pp. 92–98.
[25] Wasserman, S. R., Tao, Y. T., and Whitesides, G. M., 1989, "Structure and Reactivity of Alkylsiloxane Monolayers Formed by Reaction of Alkyltrichlorosilanes on Silicon Substrates," Langmuir, **5**, pp. 1074–1087.
[26] Wasserman, S. R., Whitesides, G. M., Tidswell, I. M., Ocko, B. M., Pershan, P. S., and Axe, J. D., 1989, "The Structure of Self-Assembled Monolayers of Alkylsiloxanes on Silicon – A Comparison of Results From Ellipsometry and Low-Angle X-Ray Reflectivity," J. Am. Chem. Soc., **111**, pp. 5852–5861.
[27] Chen, C. Y., Loch, C. L., Wang, J., and Chen, Z., 2003, "Different Molecular Structures at Polymer/Silane Interfaces Detected by SFG," J. Phys. Chem. B, **107**, pp. 10440–10445.

Downloaded 26 Apr 2012 to 128.95.104.109. Redistribution subject to ASME license or copyright; see http://www.asme.org/terms/Terms_Use.cfm